Effect of MgO doping of periodically poled lithium niobate on second-harmonic generation of femtosecond laser pulses

Junfeng Zhang, Yuping Chen,* Feng Lu, Wenjie Lu, Weirui Dang, Xianfeng Chen, and Yuxing Xia

Department of Physics, State Key Laboratory on Fiber Optics Local Area Communication Networks and Advanced Optical Communication Systems, Shanghai Jiao Tong University, 800 Dongchuan Road, Shanghai 200240, China

*Corresponding author: ypchen@sjtu.edu.cn

Received 15 May 2007; revised 3 August 2007; accepted 18 September 2007; posted 27 September 2007 (Doc. ID 83105); published 1 November 2007

We theoretically analyze type-I broadband second-harmonic generation (SHG) of femtosecond laser pulses based on a quasi-phase-matching configuration in periodically poled congruent $LiNbO_3$ (LN) and periodically poled $MgO:LiNbO_3$ (PPMgLN) (5% and 7%). Group-velocity matching (GVM) can be achieved at the fundamental waves of 1.59, 1.56, and 1.55 μm for SHG when the three types of crystals have grating periods of 22.31, 20.07, and 23.45 μm, respectively. It is found that the central wavelength of the fundamental wave for GVM will increase with the decrease of MgO doping in LN. It is concluded that the shift of the GVM central wavelength is due to the difference of MgO doping, which changes the dispersion of the crystal. Therefore, tunable and high efficiency broadband SHG of femtosecond laser pulses in a long crystal can be realized by selecting different doping rates of PPMgLN. © 2007 Optical Society of America

OCIS codes: 190.2620, 190.4400.

1. Introduction

In frequency doubling of a femtosecond laser pulse, the group-velocity (GV) mismatch between the fundamental harmonic (FH) wave and second-harmonic (SH) wave limits the nonlinear interaction as well as the spectral bandwidth, which leads to a considerable broadening of the SH pulses. The common way to maintain the broad bandwidth of the FH wave is to use a thin nonlinear material. However, the short interaction length will result in a substantial decrease in conversion efficiency because the efficiency is proportional to the square of the crystal length. Some approaches and devices have been developed to eliminate the GV mismatch. Huang *et al.* proposed an integrated device to obtain group-velocity matching (GVM) [1]. But this device is inconvenient to use because it not only has small temperature tolerance but also high optical loss due to many couplers and bends. Fujioka *et al.* generated an SH wave at 780 nm with 11 nm bandwidth under noncollinear quasi-phase-matching (QPM) geometry [2]. This scheme requires precise control of the noncollinear angle and the propagation direction, therefore making the adjustment of experiment equipment rather difficult.

QPM technology plays an essential role in frequency conversion because it can utilize large nonlinear susceptibility in the whole transparency range of nonlinear material. Various QPM materials have been investigated in past years [3–8]. Among these materials, periodically poled $MgO:LiNbO_3$ (PPMgLN) is one of the most attractive to realize GVM for second-harmonic generation (SHG) due to its high nonlinearity, relatively high damage threshold, and low coercive electric field [9–11]. In 2002, Yu *et al.* proposed a novel scheme of simultaneously attaining GVM and QPM to get broadband SHG in the com-

0003-6935/07/327792-05$15.00/0
© 2007 Optical Society of America

munication band through appropriately selecting the FH wavelength, temperature, and QPM grating period [12]. In the following year, this scheme was realized in a 10 mm long, 5% PPMgLN [13]. Realization of GVM and QPM is due to the dispersion relation of the crystals, and also it is mentioned that material dispersion can be tailored by choosing an appropriate doping level to achieve the desired GVM wavelength.

In this paper, we theoretically analyze type-I broadband QPM SHG in periodically poled congruent $LiNbO_3$ (PPCLN) and PPMgLN (5% and 7% MgO doped). In the three types with grating periods of 22.31, 20.07, and 23.45 μm, GVM can be achieved at the FH wavelength of 1.59, 1.56, and 1.55 μm, respectively. We find that the central wavelength of the fundamental wave for GVM will shift to longer wavelength with the decrease of the doping rate of MgO in $LiNbO_3$ (LN). This shift of the GVM central wavelength is owing to MgO doping in LN, which changes its dispersion relation [14]. Finally, the paper presents some parameters for frequency doubling of a femtosecond pulse laser in these crystals, and gives a comparison of the influence of the doping rates on GVM and QPM SHG.

2. Numerical Calculations

By using the d_{31} nonlinear coefficient in a z-cut crystal with the beam propagation along the x axis, first-order type-I QPM SHG in LN can be expressed as $E_y^{\omega}E_y^{\omega} \rightarrow E_z^{2\omega}$ [15], where E_i^{ω} ($i = x, y, z$) is the electric component at a frequency ω, which is parallel to the i axis of the crystal. With a small-signal approximation, the normalized SH intensity η can be expressed as

$$\eta \propto \mathrm{sinc}^2(\Delta k L/2), \tag{1}$$

where L is the crystal length and Δk is the overall phase mismatch between interactive light waves, which can be expressed by

$$\Delta k = k_z^{2\omega} - 2k_y^{\omega} - \frac{2\pi}{\Lambda_1} = \frac{4\pi(n_z^{2\omega} - n_y^{\omega})}{\lambda} - \frac{2\pi}{\Lambda_1}. \tag{2}$$

In Eq. (2), Λ_1 is the first-order QPM grating period of frequency doubling in the type-I QPM case. When the QPM grating period

$$\Lambda_1 = \frac{2\pi}{\Delta k'} = \frac{\lambda}{2(n_z^{2\omega} - n_y^{\omega})}, \tag{3}$$

is satisfied in Eq. (3), where $\Delta k' = k_z^{2\omega} - 2k_y^{\omega}$ is the wave vector mismatch, then $\Delta k = 0$.

For first-order type-I broadband QPM SHG, the dependence of the wave vector mismatch on wavelength can be derived as

$$\frac{d(\Delta k')}{d\lambda} = \frac{4\pi c}{\lambda^2}\,\delta. \tag{4}$$

Here λ is the fundamental wavelength, and $\delta = 1/v_{g_1} - 1/v_{g_2}$ is the GV walk-off parameter, with $v_{g_{1i}}$ and $v_{g_{2i}}$ being the GVs for the fundamental harmonic and the SH, respectively. If a certain local extremum $d(\Delta k')/d\lambda = 0$ of the unique dispersion can be obtained in the spectral region, the GV matching ($\delta = 0$) can be realized correspondingly. Then GVM and QPM SHG are satisfied at the same time. According to Eqs. (3) and (4), the wavelength region of satisfying GVM and QPM simultaneously is determined by the dispersion of materials. So it is possible to tune the wavelength to the desired wavelength domain by changing the MgO doping in PPMgLN.

A. Broadband Second-Harmonic Generation Grating Period

Figure 1 shows how the QPM grating period varies with the fundamental wavelength for type-I QPM broadband SHG in PPCLN and in 5% and 7% PPMgLN from 1.50 to 1.66 μm at their respective center temperatures. We set the crystal length of 1 cm in this paper for general purpose or normalization. The grating period is calculated according to the Sellmeier equations provided by [16–18].

In Fig. 1, the grating period for the type-I SHG, in three crystals reaches the maximum value around the telecommunication wavelength, where the broad bandwidth SHG can be expected. At this point, the GVM and QPM SHG are simultaneously satisfied so the GV walk-off length is theoretically infinite (GV walk-off length for the case of SHG in this paper, L_{gv}, is defined as $L_{gv} = \tau_0/|\delta|$, where τ_0 is the pulse duration of the FH wave). Therefore, SHG in expected broadband with high efficiency frequency conversion can be obtained in longer crystal length, eliminating the disadvantage of poor efficiency and bandwidth from the existing birefringence approach.

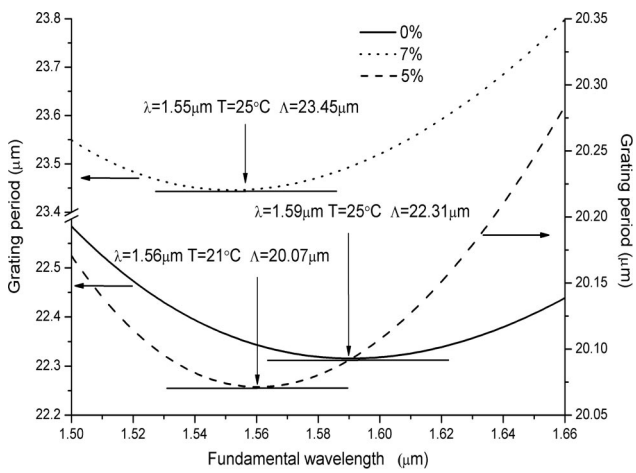

Fig. 1. Grating period versus fundamental wavelength for broadband QPM SHG. At the center temperature, the grating periods are 22.31, 20.07, and 23.45 μm at the broadband SHG center wavelengths of 1.59, 1.56, and 1.55 μm for PPCLN, 5% and 7% PPMgLN.

At 25 °C, for the 7% MgO doped PPMgLN, we draw a tangent line on the dotted curve. We can find that the grating period is 23.45 μm when the wavelength of the FH wave is 1.55 μm; that means at 25 °C and the FH wavelength of 1.55 μm, both GVM and QPM SHG without limitation of interactive length can be realized in 7% MgO doped PPMgLN with a grating period of 23.45 μm. Similarly, we are able to get the grating period and center wavelength for GVM at the center temperature for PPCLN and 5% PPMgLN. If the temperature of the 7% PPMgLN sample is changed, the dotted curve in Fig. 1 will move up or down correspondingly. For example, the dotted curve will move down and have two cross points with the tangent line as long as the sample temperature decreases. At the two cross points, QPM SHG is still satisfied while GVM is not, resulting in two QPM SHG peaks. However, once the temperature exceeds 25 °C, the dotted curve in Fig. 1 will move up and have no cross points with the tangent line. Then, neither GVM nor QPM SHG is satisfied and the SHG efficiency becomes rather low. This phenomenon is also applicable to PPCLN and 5% PPMgLN.

Figure 1 shows that the GVM wavelengths are 1.59, 1.56, and 1.55 μm for PPCLN, 5% PPMgLN, and 7% PPMgLN, respectively. We find that as the MgO doping rate increases, the GVM wavelength will drift to the shorter wavelength domain. This is because the changing of the dispersion relationship induced by MgO doping in $LiNbO_3$ affects the GVM and QPM SHG process. We will investigate this phenomenon in Subsection 2.B.

B. Shift of Group-Velocity-Matching Center Wavelength Due to Variation of MgO Doping Rate

According to the definition of $\Delta k' = k_z^{2\omega} - 2k_y^{\omega}$, we can derive Eq. (5) from Eq. (4):

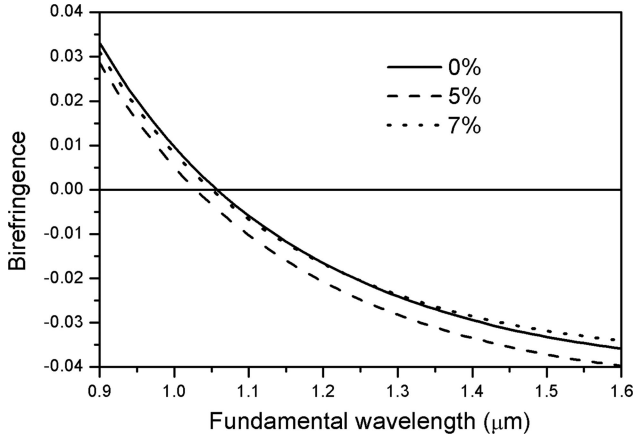

Fig. 3. Variation of birefringence ($\Delta n = n_e - n_o$) for PPCLN, 5% and 7% PPMgLN of fundamental wave versus fundamental wavelength.

$$\begin{aligned}\frac{\mathrm{d}(\Delta k')}{\mathrm{d}\lambda} &= \frac{\mathrm{d}\left(k_z^{2\omega} - 2k_y^{\omega}\right)}{\mathrm{d}\lambda} \\ &= \frac{4\pi}{\lambda^2}\left(\left(n_y^{\omega} - \lambda\frac{\mathrm{d}n_y^{\omega}}{\mathrm{d}\lambda}\right) - \left(n_z^{2\omega} - \lambda\frac{\mathrm{d}n_z^{2\omega}}{\mathrm{d}\lambda}\right)\right) \\ &= \frac{4\pi c}{\lambda^2}\,\delta. \end{aligned} \tag{5}$$

From Eq. (5), we can get the relationship between GV walk-off parameter δ (GVM parameter) and the FH wavelength in three crystals as plotted in Fig. 2. As shown in Fig. 2, GVM can be achieved at 1.59, 1.56, and 1.55 μm, respectively. At the same time, QPM SHG with the maximum broadband bandwidth and high efficiency can be obtained at a certain temperature with grating periods corresponding to the GVM wavelength. Also in Fig. 2, GVM wavelength shifts to the shorter wavelength domain as the MgO

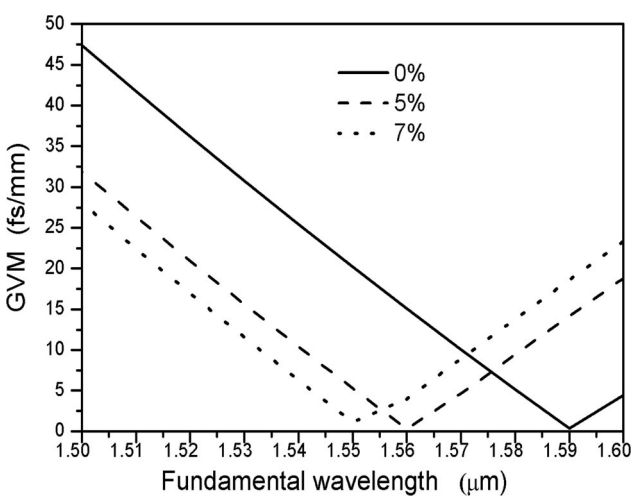

Fig. 2. GV walk-off parameter versus fundamental wavelength for PPCLN, 5% and 7% PPMgLN, in which GVM (δ = 0) can be achieved at the fundamental wavelength of 1.59, 1.56, and 1.55 μm, respectively.

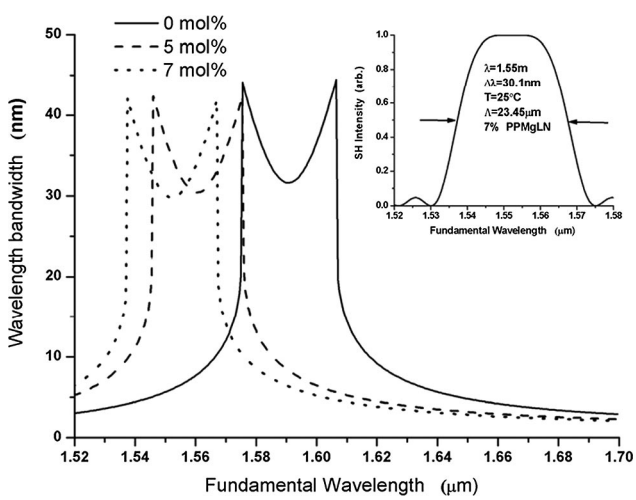

Fig. 4. Wavelength domain of SH wave. The inset corresponds to the lowest point on the dotted curve of PPMgLN. For PPCLN, 5% and 7% PPMgLN, the ranges of conversion efficiency higher than 50% are 1547–1607, 1545–1575, and 1537–1567 nm, respectively.

Table 1. Parameters of GV-Matched Broadband QPM SHG for Differently Doped MgO:LN

Crystal	Temperature (°C)	Poling Period (μm)	GVM Fundamental Wavelength (μm)	SH Bandwidth (nm)	Angle Bandwidth (°)	Temperature Bandwidth (°C)
PPCLN	25	22.31	1.59	33.2	2.94	0.53
PPMgLN (5%)	25	20.28	1.56	31.1	2.78	0.22
PPMgLN (7%)	25	23.45	1.55	30.1	2.93	0.22

doping rate increases. The results are consistent with those in Fig. 1.

Reference [14] shows that in LN crystal, Li—O bonds have influence on extraordinary refractive index (n_c), while Nb—O bonds affect the ordinary refractive index (n_o). When MgO is doped in LN and the doping rate increases, Mg ions gradually substitute Nb ions. So n_c and n_o, then the birefringence index, are altered. As shown in Fig. 3, the birefringence index and the critical phase-matching wavelength have been changed significantly as the concentration of MgO in LN varies. In fact, the effect of MgO doping on n_c and n_o illustrates how the MgO doping changes the characteristics of femtosecond pulses SHG, i.e., it alters the dispersion equations of nonlinear crystals. This theoretical result indicates that, besides the method of adjusting the temperature to change the GVM center wavelength [3,12], we can also achieve GVM of femtosecond pulse SHG at room temperature in the expected wavelength by controlling the MgO doping rates in PPMgLN. It is reported that PPMgLN with Mg ion concentration as high as 25% has been successfully fabricated [19]. Therefore, the special applications of these highly doped crystals could be investigated deeply for nonlinear optical parameter processes. For example, by selecting PPMgLN with different doping rates, we can extend the wavelength region of the femtosecond pulse in frequency doubling, the quadratic cascaded process involving SHG and DFG, or other parameter processes.

C. Effect of MgO Doping on Second-Harmonic Generation Process of Femtosecond Pulses

For the three crystals with length of 1 cm, in Fig. 4 we calculate the FWHM (full width at half-maximum) of the normalized SH conversion efficiency η at each of the broadband SHG center wavelengths from 1.50 to 1.70 μm. We find that for PPCLN, 5% and 7% PPMgLN, the ranges of conversion efficiency higher than 50% are 1547–1607, 1545–1575, and 1537–1567 nm, respectively. In Fig. 4, neglecting the GV mismatch, the wavelength domain of broadband QPM SHG shifts to the shorter wavelength. It should be noticed that two maximum points appear in Fig. 4. This phenomenon has been explained in detail by Wu *et al.* [3]. The results are suitable for continuous light sources, or nonultrashort pulse light sources (picoseconds or larger pulse duration), to achieve broadband QPM SHG. However, if we want to realize the SHG of a femtosecond pulse laser, both QPM and GVM should be taken into consideration to obtain broad bandwidth and high conversion efficiency.

In frequency doubling of a femtosecond pulse laser, adjustable broader ranges of temperature and incident angles are advantageous to obtain high efficiency and maintain the pulsed energy stability of the converted beam [20]. Consequently, we calculated the temperature bandwidth and angle bandwidth at center wavelength of broadband QPM SHG. For better comparison of QPM SHG of femtosecond pulses among these three crystals, in Table 1 we list the parameters for frequency doubling of femtosecond pulses in practical applications.

3. Conclusion

We have analyzed and compared the frequency doubling of femtosecond laser pulses in MgO differently doped LN. The doping rates greatly affect the realization of GVM for obtaining pulses with little distortion and high efficiency, i.e., significantly the walk-off length of ultrashort wave pulses to increase the interacting length of SH and FH waves. Different concentration of MgO in LN has different dispersion relation of crystals. We notice that the GVM center wavelengths shift to the shorter wavelengths as the doping rates in PPMgLN rise. This result makes it possible to choose PPMgLN with an appropriate doping rate to obtain SHG of femtosecond laser pulses in the expected wavelength domain at room temperature. With successful fabrication of highly MgO doped LN, it is possible to use these crystals to realize femtosecond pulse frequency doubling in a desired wavelength region, as well as quadratic cascaded process involving SHG and DFG, or other parameter processes. Finally, for these three crystals, we gave the GVM center wavelength, grating period, temperature, and wavelength bandwidth for frequency doubling of femtosecond laser pulses.

This research is supported by the National Natural Science Foundation of China (60407006, 60477016, and 10574092), and the National High Technology Research and Development Program (863) of China (2007AA01Z273).

References

1. J. Huang, J. R. Kurz, C. Langrock, A. M. Schober, and M. M. Fejer, "Quasi-group-velocity matching using integrated-optic structures," Opt. Lett. **29,** 2482–2484 (2004).
2. N. Fujioka, S. Ashihara, H. Ono, T. Shimura, and K. Kuroda, "Group-velocity-matched noncollinear second-harmonic gener-

ation in quasi-phase matching," J. Opt. Soc. Am. B **22,** 1283–1289 (2005).
3. R. Wu, Y. Chen, J. Zhang, X. Chen, and Y. Xia, "Broadening of the second-harmonic phase-matching bandwidth in type II periodically poled KTP," Appl. Opt. **44,** 5561–5564 (2005).
4. Y. Wang, J. Fonseca-Campos, C.-Q. Xu, S. Yang, E. A. Ponomarev, and X. Bao, "Picosecond-pulse wavelength conversion based on cascaded second-harmonic generation-difference frequency generation in a periodically poled lithium niobate waveguide," Appl. Opt. **45,** 5391–5403 (2006).
5. S. Wang, V. Pasiskevicius, J. Hellstrom, F. Laurell, and H. Karlsson, "First-order type II quasi-phase-matched UV generation in periodically poled KTP," Opt. Lett. **24,** 978–980 (1999).
6. H. Ishizuki, I. Shoji, and T. Taira, "Periodical poling characteristics of congruent MgO:$LiNbO_3$ crystals," Appl. Phys. Lett. **82,** 4062–4063 (2003).
7. M. M. J. W. van. Herpen, S. E. Bisson, and F. J. M. Harren, "Continuous-wave operation of a single-frequency optical parametric oscillator at 4–5 μm based on periodically poled $LiNbO_3$," Opt. Lett. **28,** 2497–2499 (2003).
8. G. Z. Luo, S. N. Zhu, J. L. He, Y. Y. Zhu, H. T. Wang, Z. W. Liu, C. Zhang, and N. B. Ming, "Simultaneously efficient blue and red light generations in a periodically poled $LiTaO_3$," Appl. Phys. Lett. **78,** 3006–6008 (2001).
9. I. Shoji, T. Kondo, A. Kitamoto, M. Shirane, and R. Ito, "Absolute scale of second-order nonlinear-optical coefficients," J. Opt. Soc. Am. B **14,** 2268–2294 (1997).
10. D. A. Bryan, R. Gerson, and H. E. Tomaschke, "Increased optical damage resistance in lithium niobate," Appl. Phys. Lett. **44,** 847–849 (1984).
11. A. Kuroda, S. Kurimura, and Y. Uesu, "Domain inversion in ferroelectric MgO:$LiNbO_3$ by applying electric fields," Appl. Phys. Lett. **69,** 1565–1567 (1996).
12. N. E. Yu, J. H. Ro, and M. Cha, "Broadband quasi-phase-matched second-harmonic generation in MgO-doped periodically poled $LiNbO_3$ at the communications band," Opt. Lett. **27,** 1046–1048 (2002).
13. N. E. Yu, S. Kurimura, and K. Kitamura, "Efficient frequency doubling of a femtosecond pulse with simultaneous group-velocity matching and quasi phase matching in periodically poled, MgO-doped lithium niobate," Appl. Phys. Lett. **82,** 3388–3390 (2003).
14. P. Sen, P. K. Sen, R. Bhatt, S. Kar, V. Shukla, and K. S. Bartwal, "The effect of MgO doping on optical properties of LiNbO3 single crystals," Solid State Commun. **129,** 747–752 (2004).
15. Y. Chen, X. Chen, S. Xie, X. Zeng, Y. Xia, and Y. Chen, "Polarization dependence of quasi-phase-matched second-harmonic generation in bulk periodically poled $LiNbO_3$," J. Opt. A **4,** 324–328 (2002).
16. D. H. Jundt, "Temperature-dependent Sellmeier equation for the index of refraction, n_c, in congruent lithium niobate," Opt. Lett. **22,** 1553–1555 (1997).
17. D. Zelmon, D. Small, and D. Jundt, "Infrared corrected Sellmeier coefficients for congruently grown lithium niobate and 5 mol. magnesium oxide doped lithium niobate," J. Opt. Soc. Am. B **14,** 3319–3322 (1997).
18. Casix, http://www.casix.com/product/prod_cry_linbo3.html.
19. L. J. Hu, Y. H. Chang, I. N. Lin, and S. J. Yang, "Defects of lithium niobate crystals heavily doped with MgO," J. Cryst. Growth **114,** 191–197 (1991).
20. B. Boulanger, J. P. Feve, G. Marnier, C. Bonnin, and P. Villeval, "Absolute measurement of quadratic nonlinearities from phase-matched second-harmonic generation in a single KTP crystal cut as a sphere," J. Opt. Soc. Am. B **14,** 1380–1386 (1997).